Bridging temporal gaps: Thermoluminescence (TL) thermochronology as a key to active tectonics and knickpoint migration in the San Gorgonio Pass

Ayush Joshi*[1], Nathan D. Brown[1]**, Marina Argueta[2,3] and Seulgi Moon[2]
[1]Department of Earth and Environmental Sciences, University of Texas at Arlington, Arlington, TX 76010
[2]Department of Earth, Planetary and Space Sciences, University of California, Los Angeles, Los Angeles, CA 90095-1567
[3]Department of Geology, Pomona College, Claremont, CA 91711
*ayush.joshi@uta.edu, **nathan.brown@uta.edu

1. INTRODUCTION

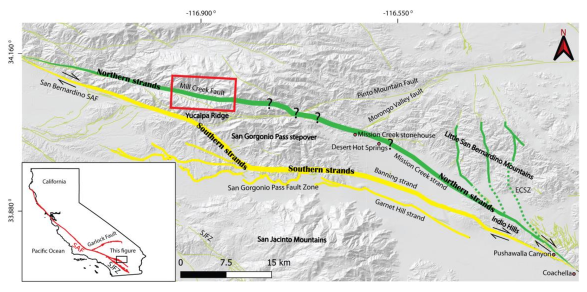

Hillshade map of the Southern San Andreas Fault depicting major fault strands in the region. The slip passing through this multistranded region is accommodated by faults along the northern (labelled in green) and southern strands (labelled in yellow). The study area is highlighted in red (modified from Beyer et al., 2018; Blisniuk et al., 2021)

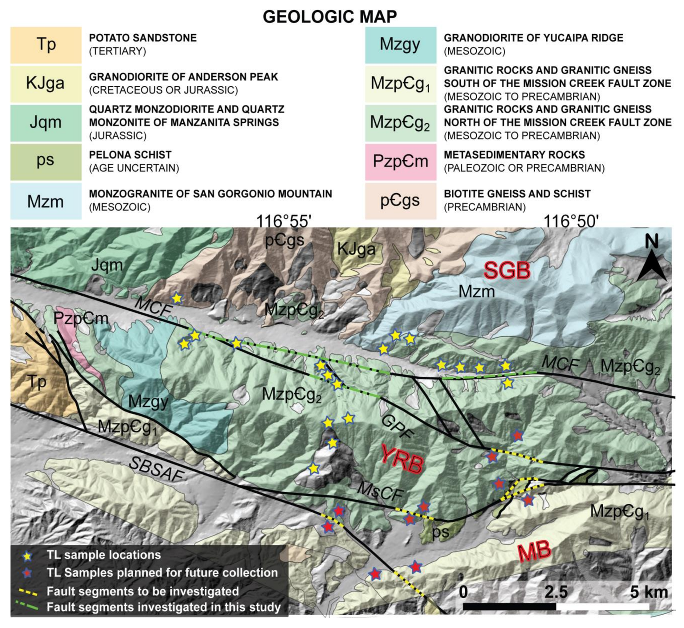

Tectonic setup of the study site. This figure was modified from a NEHRP proposal figure by Brown that adopts geologic unit mapping from Matti et al. (1983) and fault mapping from Alex Morelan's Ph.D. thesis work (unpublished).

How does slip partitioning among various fault strands in the San Gorgonio Pass (SGP) region occur?

Can systematic differences in bedrock erosion rates across active fault strands in the SGP region provide insights into spatial variability in tectonic uplift, and hence, fault activity?

Can TL thermochronology capture landscape response to millennial scale base level change?

2. TRAPPED CHARGE DATING

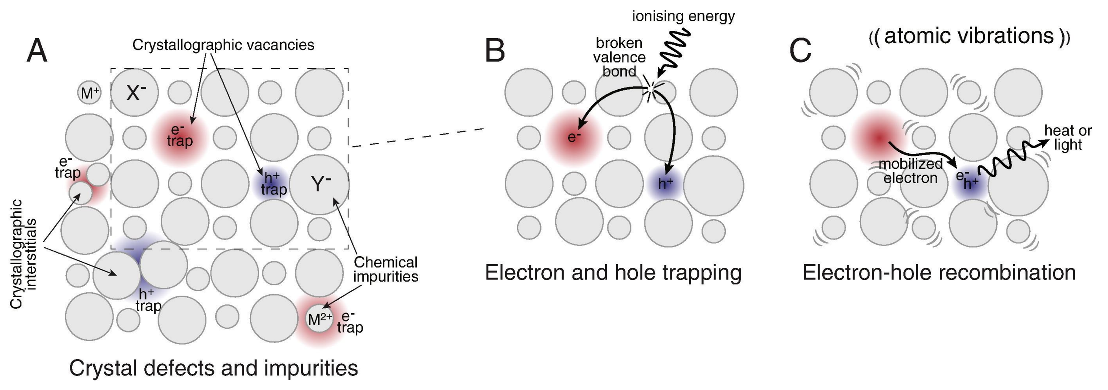

Schematic for trapped charge dating in a crystal lattice (King et al., 2016c)

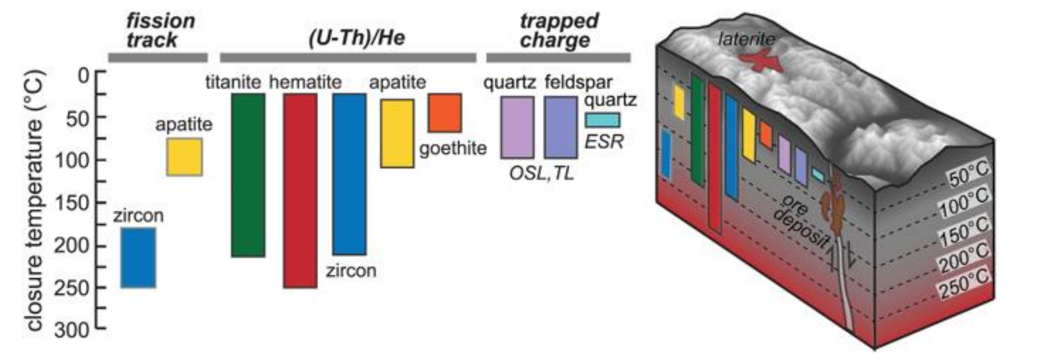

Closure temperatures for various thermochronometers within mineral systems, including Fission Track, (U-Th)/He, and trapped charge methods (Ault et al., 2019).

TL thermochronology: Ultra-low temperature dating technique that can replicate bedrock exhumation history, using feldspar's luminescence signals to probe thermal history over 10^4 to 10^5 years.

Role of geothermal heat: Geothermal heat affects the accumulation of the luminescence signal in feldspar. With the TL signal, we can record the bedrock's thermal history during the latter stages of its exhumation, spanning tens to hundreds of meters, which is crucial for understanding topographical changes due to tectonic and erosional processes.

Kinetic parameters and cooling age: Thermal experiments are used to constrain kinetic parameters that regulate charge growth and decay within feldspar.

3. TL THERMOCHRONOLOGY WORKFLOW

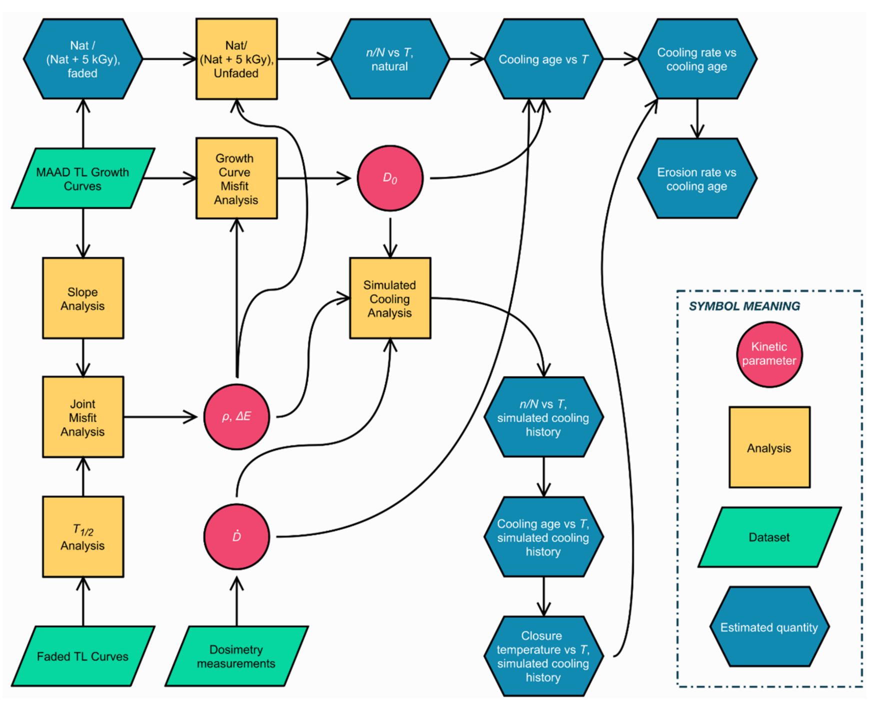

$n(r')$ and $N(r')$ are the concentrations (m^{-3}) of occupied and total trapping sites respectively

$\dot{D}$ is the geologic dose rate (Gy/ka); D_0 is the characteristic dose of saturation (Gy)is the geologic dose rate (Gy/ka); D_0 is the characteristic dose of saturation (Gy)

ΔE is the activation energy difference between the ground and excited states (eV)

T is the absolute temperature of the sample (K)

k_B is the Boltzmann constant (eV/K)

s is the frequency factor (s^{-1})

$P(r')$ is the tunnelling probability at some distance r' (s^{-1}) and is a function of dimensionless recombination centre density (ρ')

Governing Equation:

$$\frac{dn(r')}{dt} = \frac{\dot{D}}{D_0}\left(N(r') - n(r')\right) - n(r')\exp\left(-\frac{\Delta E}{k_B T}\right)\frac{P(r')s}{P(r') + s}$$

4. EROSIONAL CONTRAST BETWEEN THE WESTERN AND EASTERN MILL CREEK FAULT SEGMENTS

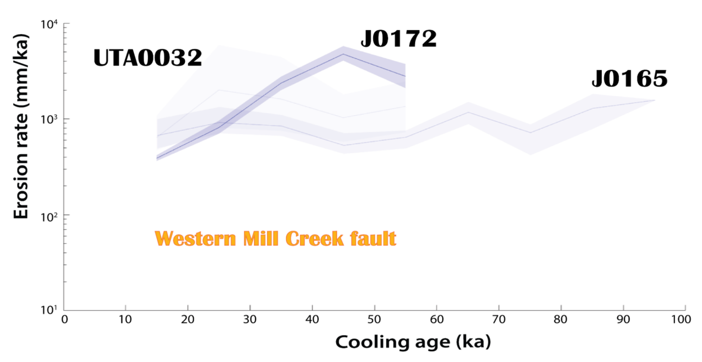

Samples near the eastern Mill Creek fault are eroding at a faster pace compared to the western Mill Creek fault.

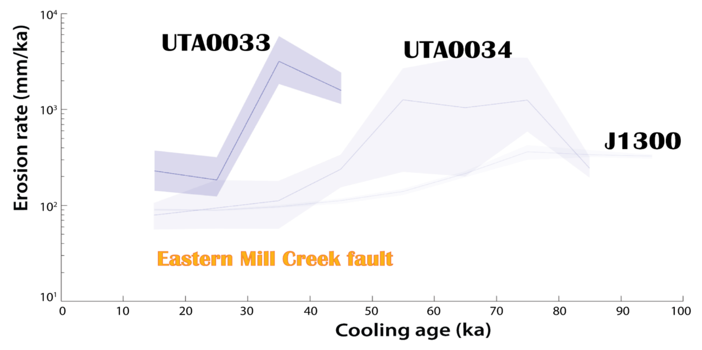

Concentration of high erosion rates along the western Mill Creek fault might point towards a more localised control on bedrock erodibility.

5. POSITIVE CORRELATION OF TL EROSION RATES WITH RELIEF

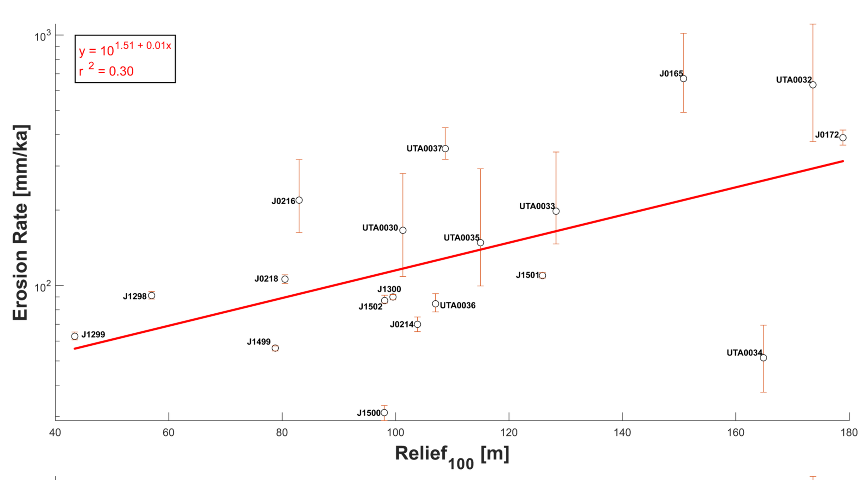

Erosion rates from TL thermochronology show a weak positive correlation with 100 m-radius relief, with an R^2 value of 0.30.

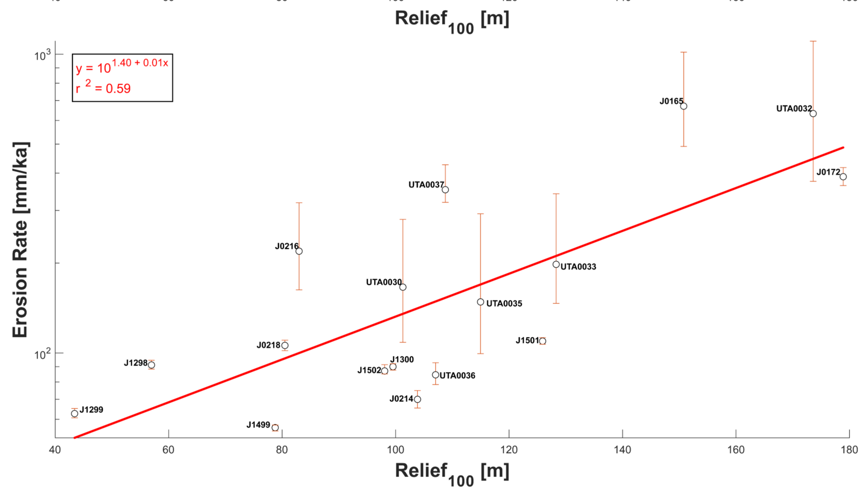

Excluding samples J1500 and UTA0034, which show anomalously low erosion rates despite high relief, improves the correlation substantially, yielding an R^2 value of 0.59 and indicating a stronger positive relationship.

6. TRANSIENT RESPONSE TO A CHANGE IN BASE LEVEL IN THE MILL CREEK CATCHMENT

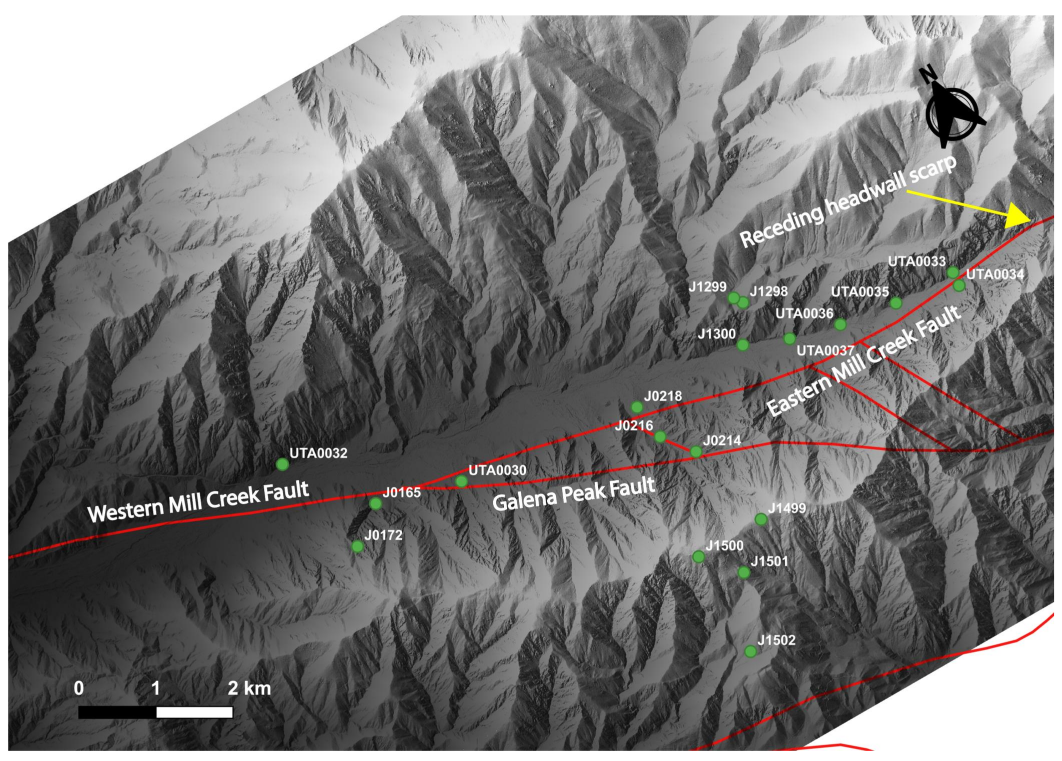

Hillshade map of the Mill Creek catchment depicting the tectonic architecture and sampling locations

Lateral knickpoint migration rate is estimated as:

$$R = \frac{Distance(D)}{Age(A)}$$

where, 'D' represents the distance between the selected sample and the headwall scarp and 'A' is the cooling age at which sample exhibits a drop in erosion rate

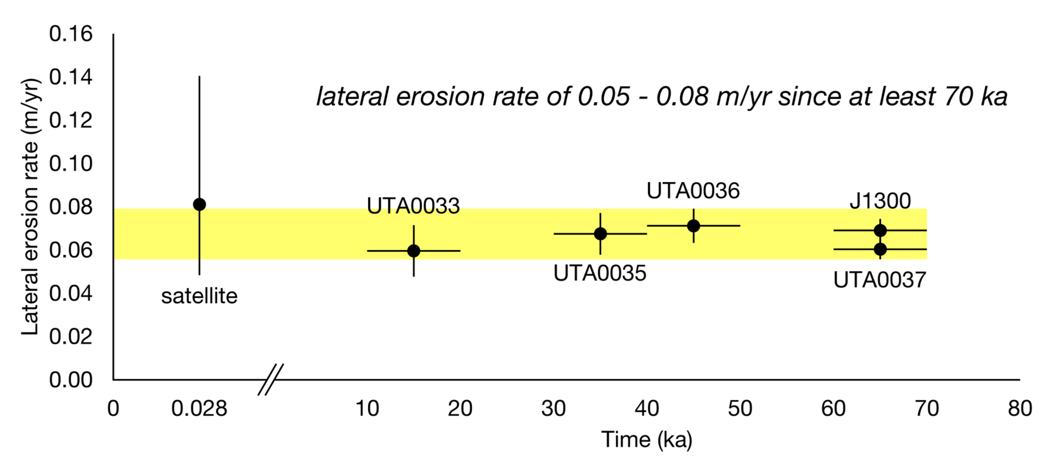

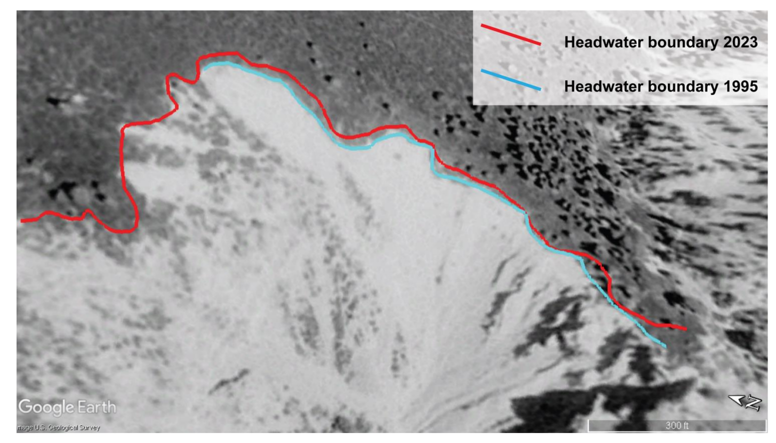

Receding headwall scarp boundary between 1995 and 2023

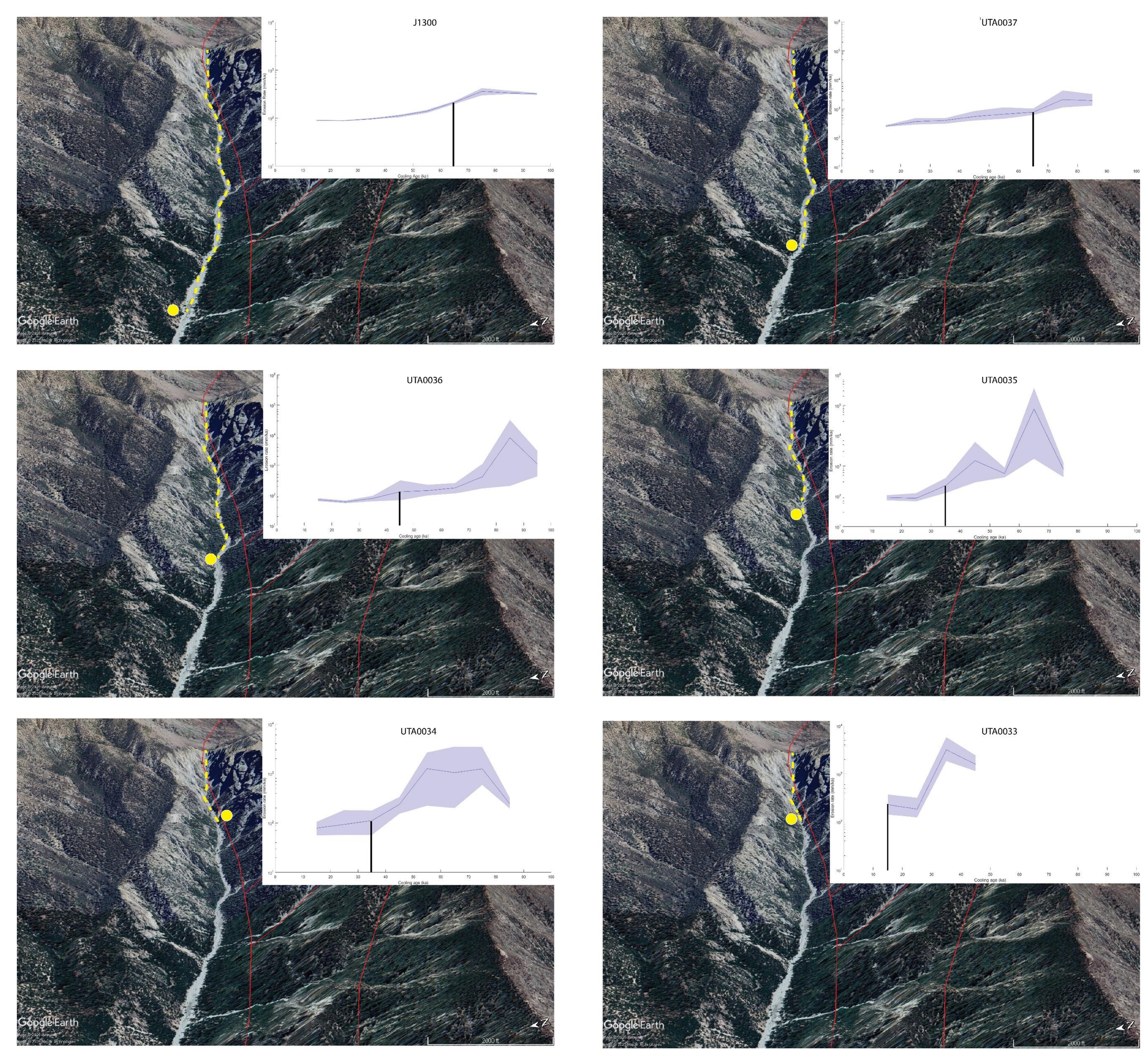

Samples collected near the headwall scarp are marked with yellow circles. The distance 'D' from each sample to the scarp is shown with a yellow dashed line. The vertical black line marks the cooling age corresponding to a sharp decrease in erosion rate

7. BIG TAKEAWAYS

The difference in erosion rates between the eastern and western Mill Creek faults suggests that the Galena Peak Fault may be accommodating slip transferred to the western Mill Creek Fault, bypassing the eastern segment.

Systematic variations in erosion rates across a fault strand may be influenced by local factors such as bedrock erodibility and spatial differences in bedrock geology. Further investigation is needed to determine the extent to which these geological factors affect TL-derived erosion rates.

A transient response to a change in base level is recorded within the catchment, evidenced by the systematic upstream migration of an erosional wave observed in the erosion history plots. These erosion rates fall within one sigma of the lateral headwall erosion rate derived from 28 years of satellite data.

8. REFERENCES

Ault, A. K., Gautheron, C., & King, G. E. (2019). Innovations in (U–Th)/He, fission track, and trapped charge thermochronometry with applications to earthquakes, weathering, surface-mantle connections, and the growth and decay of mountains. Tectonics, 38. https://doi.org/10.2029/2018TC005312

Beyer, J., Cooke, M. L., & Marshall, S. T. (2018). Sensitivity of deformation to activity along the Mill Creek and Mission Creek strands of the southern San Andreas fault. Geosphere, 14(6), 2296–2310. https://doi.org/10.1130/GES01666.1

Blisniuk, K., Scharer, K., Sharp, W. D., Burgmann, R., Amos, C., & Rymer, M. (2021). A revised position for the primary strand of the Pleistocene-Holocene San Andreas fault in southern California. In Sci. Adv (Vol. 7). https://www.science.org

King, G. E., Guralnik, B., Valla, P. G., & Herman, F. (2016). Trapped-charge thermochronometry and thermometry: A status review. *Chemical Geology, 446*, 3–17. https://doi.org/10.1016/j.chemgeo.2016.08.023

Matti, J. C., Cox, B. F., & Iverson, S. R. (1983). Mineral resource potential map of the Raywood Flat Roadless Area, San Bernardino and Riverside Counties, California (U.S. Geological Survey Miscellaneous Field Studies Map MF-1563-A). U.S. Geological Survey. Scale 1:62,500.